




## ORIGINAL RESEARCH ARTICLE

# Growth differentiation factor 11 locally controls anterior–posterior patterning of the axial skeleton

Joonho Suh<sup>1</sup>  | Je-Hyun Eom<sup>1</sup> | Na-Kyung Kim<sup>1</sup> | Kyung Mi Woo<sup>1</sup> |  
Jeong-Hwa Baek<sup>1</sup> | Hyun-Mo Ryoo<sup>1</sup>  | Se-Jin Lee<sup>2,3</sup> | Yun-Sil Lee<sup>1</sup> 

<sup>1</sup>Department of Molecular Genetics and Dental Pharmacology, School of Dentistry and Dental Research Institute, Seoul National University, Seoul, Republic of Korea

<sup>2</sup>The Jackson Laboratory, Farmington, Connecticut

<sup>3</sup>Department of Genetics and Genome Sciences, School of Medicine, University of Connecticut, Farmington, Connecticut

**Correspondence**

Se-Jin Lee, Department of Genetics and Genome Sciences, School of Medicine, University of Connecticut, 263 Farmington Avenue, Farmington, CT 06032, USA.  
Email: sejlee@uchc.edu

Yun-Sil Lee, Department of Molecular Genetics and Dental Pharmacology, School of Dentistry and Dental Research Institute, Seoul National University, Bldg 86/Rm 405, 1 Gwanak-ro, Gwanak-gu, Seoul 08826, Republic of Korea.  
Email: yunlee@snu.ac.kr

**Funding information**

Research Resettlement Fund for the new faculty of Seoul National University; National Research Foundation of Korea, Grant/Award Number: NRF-2018R1D1A1B07045334

**Abstract**

Growth and differentiation factor 11 (GDF11) is a transforming growth factor  $\beta$  family member that has been identified as the central player of anterior–posterior (A–P) axial skeletal patterning. Mice homozygous for *Gdf11* deletion exhibit severe anterior homeotic transformations of the vertebrae and craniofacial defects. During early embryogenesis, *Gdf11* is expressed predominantly in the primitive streak and tail bud regions, where new mesodermal cells arise. On the basis of this expression pattern of *Gdf11* and the phenotype of *Gdf11* mutant mice, it has been suggested that GDF11 acts to specify positional identity along the A–P axis either by local changes in levels of signaling as development proceeds or by acting as a morphogen. To further investigate the mechanism of action of GDF11 in the vertebral specification, we used a *Cdx2-Cre* transgene to generate mosaic mice in which *Gdf11* expression is removed in posterior regions including the tail bud, but not in anterior regions. The skeletal analysis revealed that these mosaic mice display patterning defects limited to posterior regions where *Gdf11* expression is deficient, whereas displaying normal skeletal phenotype in anterior regions where *Gdf11* is normally expressed. Specifically, the mosaic mice exhibited seven true ribs, a pattern observed in wild-type (*wt*) mice (vs. 10 true ribs in *Gdf11*<sup>−/−</sup> mice), in the anterior axis and nine lumbar vertebrae, a pattern observed in *Gdf11* null mice (vs. six lumbar vertebrae in *wt* mice), in the posterior axis. Our findings suggest that GDF11, rather than globally acting as a morphogen secreted from the tail bud, locally regulates axial vertebral patterning.

**KEYWORDS**

*Cdx2-Cre*, GDF11, skeletal patterning, tail bud

## 1 | INTRODUCTION

Vertebrates, despite varying remarkably in body shape and size, share highly conserved developmental mechanisms regulating body segment

positioning from head to tail (Mallo, 2018). During the process of skeletal patterning along the anterior–posterior (A–P) axis, coordinated cell signaling events induce sequential addition of new tissue from progenitors at the posterior end of an embryo, eventually forming the

-----  
This is an open access article under the terms of the Creative Commons Attribution-NonCommercial-NoDerivs License, which permits use and distribution in any medium, provided the original work is properly cited, the use is non-commercial and no modifications or adaptations are made.

© 2019 The Authors *Journal of Cellular Physiology* Published by Wiley Periodicals, Inc.

axial skeleton composed of the skull, vertebral column, and thoracic cage (Wellik, 2007; Wilson, Olivera-Martinez, & Storey, 2009; Wymeersch et al., 2016). While vertebrae and ribs develop from adjacent pairs of somites, their positional information is determined in the presomitic mesoderm region before the actual formation of nascent somites (Carapuco, Novoa, Bobola, & Mallo, 2005; Kieny, Mauger, & Sengel, 1972; Nowicki & Burke, 2000; Saga & Takeda, 2001). Such positional information is thought to be provided by morphogens, or signaling molecules secreted from the signaling center, which acts at long range in a concentration-dependent manner to control specific combinatorial expressions of *Hox* genes, ensuring proper body patterning of developing embryos (Schilling, Nie, & Lander, 2012; Tickle, Summerbell, & Wolpert, 1975).

Growth and differentiation factor 11 (GDF11), a vertebrate-conserved transforming growth factor  $\beta$  (TGF- $\beta$ ) family member also known as bone morphogenetic protein 11 (BMP11), has been identified as the key molecule that determines positional identity of the axial skeleton by modulating *Hox* gene expression (Gamer et al., 1999; Jurberg, Aires, Varela-Lasheras, Novoa, & Mallo, 2013; Matsubara et al., 2017; McPherron, Lawler, & Lee, 1999). Mice homozygous for *Gdf11* deletion are perinatally lethal and display patterning defects characterized by anteriorly directed transformations of the vertebral column, leading to the extended trunk and shortened tail. Unlike normal mice that represent 13 thoracic, six lumbar vertebrae, and seven true (vertebrosternal) ribs, *Gdf11* null mice display 18 thoracic, nine lumbar vertebrae, and 10 true ribs (McPherron et al., 1999). Conversely, mice lacking GDF-associated serum protein 2, which results in hyperactivation of GDF11, exhibit posteriorly directed vertebral transformations, highlighting the critical role of GDF11 in regulating axial skeletal patterning (Lee & Lee, 2013).

GDF11 has been shown to act upstream of *Hox* genes to specify vertebral identity along the A-P axis (Aires et al., 2016; Mallo, 2018; Matsubara et al., 2017). In *Gdf11* null mice, posterior (located closer to 5' end of a chromosome) *Hox* gene expression domains are shifted posteriorly whereas anterior (located closer to 3' end of a chromosome) *Hox* gene expression domains are expanded, causing alterations in the vertebral formula (Jurberg et al., 2013; Liu, 2006; McPherron et al., 1999). In addition, ectopic expression of *Gdf11* by electroporation in a chick embryo induces anterior displacement of posterior *Hox* gene expression domains (Liu, 2006), suggesting that GDF11 likely acts to repress anterior *Hox* gene expression whereas stimulating posterior *Hox* gene expression (Mallo, 2018).

In mouse embryos, *Gdf11* is expressed around E8.0 in the primitive streak region and is predominantly expressed in the tail bud at E9.5, a crucial period for axial patterning (McPherron et al., 1999; Nakashima, Toyono, Akamine, & Joyner, 1999; Tam & Tan, 1992). Whether GDF11 acts locally or as a morphogen to specify positional identity is unknown. To examine the mode of action of GDF11 in skeletal patterning, we generated mosaic mice in which *Gdf11* expression is removed only in posterior tissues including the tail bud. More specifically, we used a *Cdx2-Cre* transgene, which is expressed as early as E3.5 and notably expressed in posterior regions by E8.5 (Hinoi et al., 2007; Silberg, Swain, Suh, & Traber, 2000), to target recombination specifically in the

caudal region of embryos carrying a floxed *Gdf11* allele. Here, we demonstrate that mosaic mice lacking *Gdf11* expression in posterior regions display abnormal skeletal patterning limited to the regions where *Gdf11* gene is removed, suggesting that GDF11 does not act globally as a morphogen secreted from the tail bud, but acts locally to control axial skeletal patterning.

## 2 | MATERIALS AND METHODS

### 2.1 | Mice

All animal studies were approved by the Institutional Animal Care and Use Committees at Seoul National University. Generation of *Gdf11* conditional knockout mice has been previously described (McPherron, Huynh, & Lee, 2009). To analyze the effect of *Cdx2-Cre* on *Gdf11<sup>flox/flox</sup>* mice, *Cdx2-Cre* transgenic male mice (Stock No. 009350), purchased from the Jackson Laboratory (Bar Harbor, ME), were first mated with *Gdf11<sup>flox/flox</sup>* female mice. Subsequently, *Cdx2-Cre; Gdf11<sup>flox/+</sup>* males were mated with *Gdf11<sup>flox/flox</sup>* females to obtain *Cdx2-Cre; Gdf11<sup>flox/flox</sup>* mice for analysis. *Gdf11* conditional knockout mice were also crossed to *Ella-Cre* transgenic female mice to generate mice heterozygous for the deletion allele (*Gdf11<sup>+/-</sup>*), and *Gdf11<sup>+/-</sup>* mice were intercrossed to generate *Gdf11<sup>-/-</sup>* mice. Because both *Cdx2-Cre; Gdf11<sup>flox/flox</sup>* and *Gdf11<sup>-/-</sup>* mice were perinatal lethal, the skeletal analysis was performed at P0. *Igs1<sup>CKI-mitoGFP/+</sup>* mice were kindly provided by Max A. Tischfield and Jeremy Nathans. All mice were maintained on a C57BL/6 background.

### 2.2 | Whole-mount in situ hybridization

E9.5 embryos were prepared and stained using digoxigenin-labeled *Gdf11* probes as previously described (McPherron et al., 1999). Briefly, embryos were hybridized at 65°C overnight, washed, and incubated with 1:4000 dilution of alkaline phosphatase-conjugated antibody (Sigma) at 4°C overnight. The color reaction was performed with nitro blue tetrazolium/5-bromo-4-chloro-3-indolyl-phosphate (Sigma).

### 2.3 | Skeletal staining

Newborn mice were prepared and stained using Alcian blue/Alizarin red solution as previously mentioned (McPherron et al., 1999). In short, mice were skinned, eviscerated, fixed, and dehydrated in ethanol and acetone. Subsequently, mice were stained for 36 hr at 37°C with a solution containing 0.003% Alizarin red (Sigma), 0.0045% Alcian blue (Sigma), and 10% acetic acid in ethanol. Finally, mice were incubated in 1% potassium hydroxide for 4 days and gradually transferred to glycerol. Photos were taken using a stereomicroscope (Zeiss) and AxioVision software (Zeiss).

### 2.4 | Micro-computed tomography

Newborn mouse skulls and vertebrae were scanned using inspeXio SMX-90CT (Shimadzu) with pixel sizes of 25 and 45  $\mu\text{m}$ , respectively at 90 kV and 110  $\mu\text{A}$ . Images were reconstructed and

displayed using a manufacturer-provided software TRI/3D-BON (RATOC System).

## 2.5 | Fluorescence microscopy

Green fluorescent protein (GFP)-positive regions of E9.5 *Cdx2-Cre; Gdf11<sup>flox/+</sup>; Igs1<sup>CKI-mitoGFP/+</sup>* embryos and newborn *Cdx2-Cre; Gdf11<sup>flox/flox</sup>; Igs1<sup>CKI-mitoGFP/+</sup>* mice were visualized using Axio Observer Z1 (Zeiss) and Zen software (Zeiss).

## 3 | RESULTS

### 3.1 | *Gdf11* expression is eliminated in caudal regions of the mosaic embryos

Using a *Cdx2-Cre* transgene in conjunction with a floxed *Gdf11* allele, we produced *Cdx2-Cre; Gdf11<sup>flox/flox</sup>* mosaic mice in which *Gdf11* expression is eliminated in posterior but not in anterior regions. To confirm the deletion of *Gdf11* expression specific to *Cdx2-Cre* expressing regions, we performed whole-mount in situ hybridization for *Gdf11* expression in E9.5 embryos. In line with previous reports (McPherron et al., 1999; Nakashima et al., 1999), *Gdf11* expression was detected predominantly in the tail bud, mildly along with the dorsal tissues, and craniofacial regions in wild-type (wt) embryos. However, in *Cdx2-Cre; Gdf11<sup>flox/flox</sup>* embryos, *Gdf11* expression was absent

specifically in the tail bud and posterior dorsal regions (Figure 1a). To visualize *Cdx2-Cre* transgene action, we utilized *Igs1<sup>CKI-mitoGFP/+</sup>* conditional knock-in mice to induce *Cdx2-Cre*-mediated recombination of a floxed stop cassette to enable GFP expression exclusively in mitochondria of *Cdx2-Cre*-positive cells (Agarwal et al., 2017). As expected, fluorescence imaging of *Cdx2-Cre; Gdf11<sup>flox/+</sup>; Igs1<sup>CKI-mitoGFP/+</sup>* embryos at E9.5 revealed GFP expression only in posterior regions corresponding to those lacking *Gdf11* expression in *Cdx2-Cre; Gdf11<sup>flox/flox</sup>* embryos (Figure 1b). Newborn *Cdx2-Cre; Gdf11<sup>flox/flox</sup>* and *Gdf11<sup>-/-</sup>* mice displayed indistinguishable outward appearance, both displaying extended torso and truncated tail (Figure 1c). Both mice also exhibited perinatal lethality although *Cdx2-Cre; Gdf11<sup>flox/flox</sup>* mice tended to live slightly longer. Analysis of GFP expression in newborn *Cdx2-Cre; Gdf11<sup>flox/flox</sup>; Igs1<sup>CKI-mitoGFP/+</sup>* mice once again confirmed that *Cdx2-Cre* action is limited to posterior tissues of the conditional knockout mice (Figure 1d).

### 3.2 | Mosaic mice display skeletal patterning defects limited to posterior regions

Normal mice represent the vertebral formula of seven cervical, 13 thoracic, six lumbar, and seven true ribs. However, mutation in *Gdf11* results in anteriorly directed homeotic transformations of vertebrae and ribs in a dose-dependent manner as *Gdf11<sup>-/-</sup>* mice display 18 thoracic, nine lumbar, and 10 true ribs, and *Gdf11<sup>+/-</sup>* mice display 14 thoracic, six lumbar, and eight true ribs (Lee & Lee,

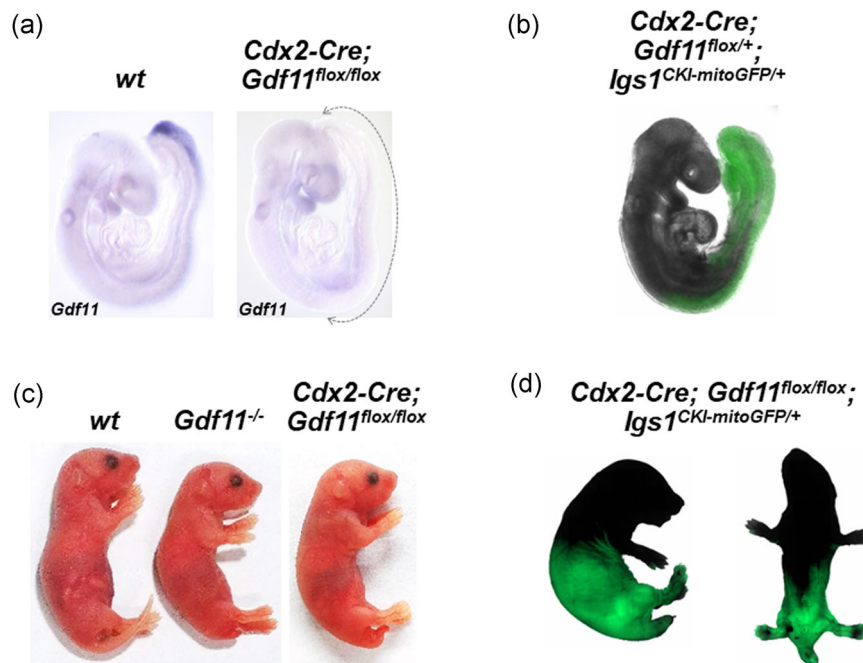


**FIGURE 1** *Gdf11* expression is removed in posterior regions of *Cdx2-Cre; Gdf11<sup>flox/flox</sup>* mice. (a) Whole-mount in situ hybridization of mouse embryos at E9.5. *Gdf11* expression patterns of wt and *Cdx2-Cre; Gdf11<sup>flox/flox</sup>* embryos are shown. Dashed line with arrow heads indicates posterior regions that lack *Gdf11* expression in a *Cdx2-Cre; Gdf11<sup>flox/flox</sup>* embryo. (b) Cells expressing *Cdx2-Cre* are marked by GFP expression in *Cdx2-Cre; Gdf11<sup>flox/+</sup>; Igs1<sup>CKI-mitoGFP/+</sup>* embryo at E9.5. (c) Newborn wt, *Gdf11<sup>-/-</sup>*, and *Cdx2-Cre; Gdf11<sup>flox/flox</sup>* pups. Both *Gdf11<sup>-/-</sup>* and *Cdx2-Cre; Gdf11<sup>flox/flox</sup>* mice display extended torso and truncated tails. (d) Area expressing *Cdx2-Cre* is labeled by GFP expression in newborn *Cdx2-Cre; Gdf11<sup>flox/flox</sup>; Igs1<sup>CKI-mitoGFP/+</sup>* mouse, and displayed laterally and ventrally. GFP, green fluorescent protein; wt, wild-type [Color figure can be viewed at [wileyonlinelibrary.com](http://wileyonlinelibrary.com)]

2013; McPherron et al., 1999). Although newborn *Cdx2-Cre; Gdf11<sup>flx/flx</sup>* share identical external appearance with *Gdf11<sup>-/-</sup>* mice, further examination demonstrated that they exhibit dissimilar skeletal patterns. In detail, Alcian blue/Alizarin red staining and micro-computed tomography (micro-CT) analysis of newborn mice revealed that while both *Cdx2-Cre; Gdf11<sup>flx/flx</sup>* and *Gdf11<sup>-/-</sup>* mice display nine lumbar vertebrae, *Cdx2-Cre; Gdf11<sup>flx/flx</sup>* and *Gdf11<sup>-/-</sup>* mice display 15 and 18 thoracic vertebrae, respectively (Figures 2a,c and S1 and Table 1), showing milder defects in thoracic

vertebrae of the mosaic mice. In anterior regions, however, *Cdx2-Cre; Gdf11<sup>flx/flx</sup>* mice exhibited normal phenotype, displaying seven true ribs, unlike *Gdf11<sup>-/-</sup>* mice that expressed 10 true ribs (Figure 2b,c and Table 1). Likewise, both *Cdx2-Cre; Gdf11<sup>flx/+</sup>* and *Gdf11<sup>+/-</sup>* mice exhibited 14 thoracic and six lumbar vertebrae (Figure 2a), but only *Cdx2-Cre; Gdf11<sup>flx/+</sup>* mice represented normal true ribs (Figure 2b). To summarize, in anterior regions where *Gdf11* is not targeted, *Cdx2-Cre; Gdf11<sup>flx/flx</sup>* mice display normal skeletal patterns but in posterior regions where *Gdf11* is targeted,

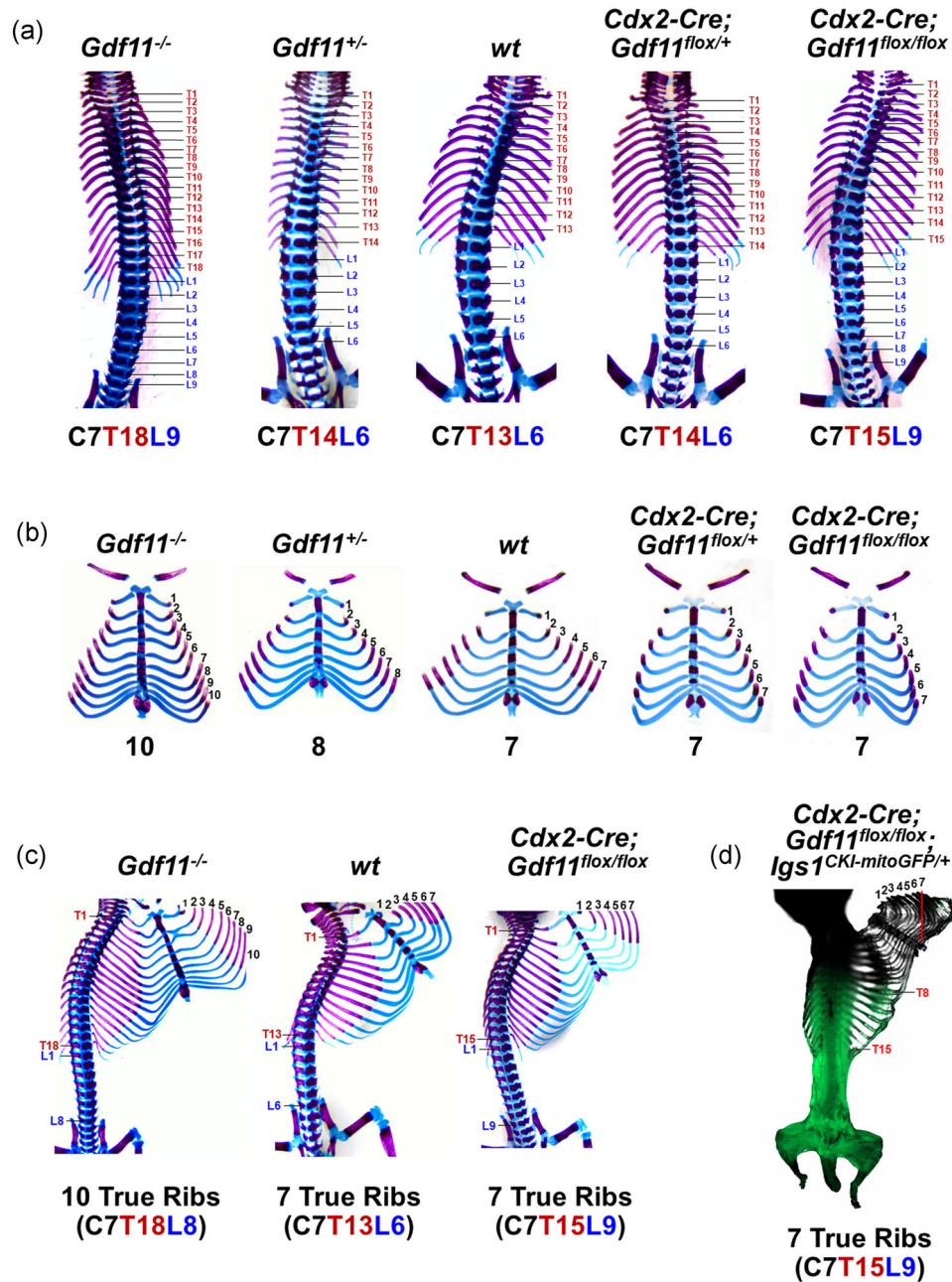


**FIGURE 2** *Cdx2-Cre; Gdf11<sup>flx/flx</sup>* mice display abnormal skeletal patterning limited to posterior regions where *Gdf11* expression is removed. (a–c) Alcian blue/Alizarin red staining of vertebral columns and vertebrosternal (true) ribs of newborn mice. True ribs attached to vertebral columns are shown in (c). Note that *Cdx2-Cre; Gdf11<sup>flx/flx</sup>* mice exhibit extended lumbar observed in *Gdf11<sup>-/-</sup>* mice but display normal true ribs. (d) Cells expressing *Cdx2-Cre* are marked by GFP expression in newborn *Cdx2-Cre; Gdf11<sup>flx/flx</sup>; Igs1<sup>CKI-mitoGFP/+</sup>* mouse. Red line points to the last (seventh) true rib. GFP, green fluorescent protein; wt, wild-type [Color figure can be viewed at [wileyonlinelibrary.com](http://wileyonlinelibrary.com)]



**TABLE 1** Skeletal analysis of wt, *Gdf11*<sup>-/-</sup>, and *Cdx2-Cre; Gdf11*<sup>flox/flox</sup> mice

Cdx2-Cre Gdf11	Genotypes of mutant mice						
	- +/+	- +/-	- -/-	- flox/+	- flox/flox	+ flox/+	+ flox/flox
N	10	13	9	17	11	14	27
Palate							
Intact	10	13	3	17	11	14	27
Cleft	-	-	6	-	-	-	-
Anterior tuberculi on no. vertebrae							
C6	10	13	8	17	11	14	27
C7	-	-	1	-	-	-	-
Attached ribs							
7	10	-	-	17	11	14	26
8	-	13	-	-	-	-	1
9	-	-	-	-	-	-	-
10	-	-	8	-	-	-	-
11	-	-	1	-	-	-	-
Total no. of thoracic vertebrae							
13	10	-	-	17	11	-	-
14	-	13	-	-	-	14	-
15	-	-	-	-	-	-	17
16	-	-	-	-	-	-	10
17	-	-	2	-	-	-	-
18	-	-	7	-	-	-	-
Total No. of lumbar vertebrae							
5	-	-	-	3	9	4	-
5/6	-	-	-	3	-	-	-
6	10	13	-	11	2	10	-
6/7	-	-	-	-	-	-	-
7	-	-	-	-	-	-	1
7/8	-	-	-	-	-	-	-
8	-	-	6	-	-	-	13
8/9	-	-	-	-	-	-	2
9	-	-	3	-	-	-	11

Abbreviation: wt, wild-type.

*Cdx2-Cre; Gdf11*<sup>flox/flox</sup> mice present anteriorly directed homeotic transformations, developing nine lumbar vertebrae, similar to what is observed in *Gdf11*<sup>-/-</sup> mice (Figures 2c and S1). In addition, fluorescence imaging of newborn *Cdx2-Cre; Gdf11*<sup>flox/flox</sup>; *Igs1*<sup>CKI-mitoGFP/+</sup> mice demonstrated that patterning defects arise below eighth thoracic vertebra, where *Gdf11* deletion is visualized by GFP expression, but not above eighth thoracic vertebra where *Gdf11* is expressed normally (Figure 2d), suggesting that locally expressed GDF11, not GDF11 secreted from the tail bud, defines positional identity in the axial skeleton.

### 3.3 | *Gdf11* null mice, but not the mosaic mice, exhibit craniofacial defects

The palate, which separates the oral and nasal cavity, starts to develop around E10.5 in the mouse embryo as the medial nasal processes fuse with maxillary processes to form the primary palate. Subsequently, palatal outgrowths emerge from the maxillary processes, forming the secondary palate, and expand vertically to become palatal shelves, which begin to fuse around E15 (Bush & Jiang, 2012; Funato, Nakamura, & Yanagisawa, 2015). Interference of these events by genetic or environmental factors can lead to the

formation of a cleft palate. GDF11 has been shown to play an essential role in normal craniofacial development as *Gdf11* is notably expressed in craniofacial regions at E9.5 (Figure 1a) and E10.5 (Nakashima et al., 1999), and *Gdf11*<sup>-/-</sup> mice exhibit a cleft palate with high penetrance (Lee & Lee, 2013, 2015; McPherron et al., 1999). Likewise, our micro-CT and Alcian blue/Alizarin red staining analysis revealed that over 60% of newborn *Gdf11*<sup>-/-</sup> mice were born with a cleft palate accompanied by the wide spacing between the pterygoid processes. However, no craniofacial defects were observed in *Cdx2-Cre; Gdf11*<sup>flox/flox</sup> mice that displayed normal palate formation (Figure 3a,b and Table 1). In fact, normal *Gdf11* expression was detected in craniofacial regions of *Cdx2-Cre; Gdf11*<sup>flox/flox</sup> mouse embryos (Figure 1a), suggesting that GDF11 locally contributes to proper craniofacial development.

## 4 | DISCUSSION

Mice deficient in *Gdf11* represent one of the most severe axial skeleton patterning defects, marking GDF11 as the pivotal regulator of vertebral skeleton segmentation along the A-P axis. Specifically, GDF11 has been identified as a secreted signaling molecule of the TGF- $\beta$  family

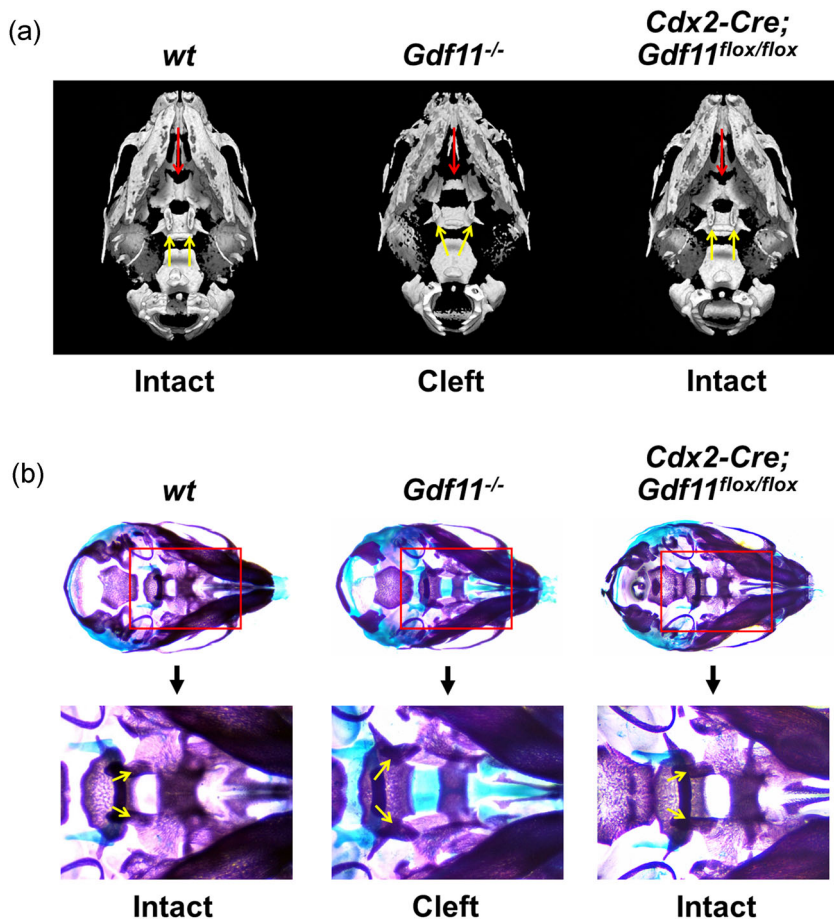


**FIGURE 3** Craniofacial defects are observed in *Gdf11<sup>-/-</sup>* mice, but not in *Cdx2-Cre; Gdf11<sup>flox/flox</sup>* mice. (a) Representative micro-CT images of newborn mouse skulls shown ventrally. Red arrows point to palatine bones, and yellow arrows indicate pterygoid processes. Note that cleft palate is observed only in *Gdf11<sup>-/-</sup>* mice. (b) Alcian blue/Alizarin red staining of newborn skulls. Boxed regions are shown at higher magnification. Yellow arrows indicate pterygoid processes. Cleft palate is observed in *Gdf11<sup>-/-</sup>* mice, but not in *Cdx2-Cre; Gdf11<sup>flox/flox</sup>* mice. micro-CT, micro-computed tomography; wt, wild-type [Color figure can be viewed at [wileyonlinelibrary.com](http://wileyonlinelibrary.com)]

predominantly expressed in the tail bud of a developing embryo. This led to the concept that the tail bud acts as a signaling center to secrete GDF11, which behaves as a morphogen to specify the vertebral formula (McPherron et al., 1999). However, *Gdf11* expression is also detected

outside the tail bud along the dorsal regions, although less prominently compared with that observed in the tail bud (Figure 1a), and whether GDF11 originated from non-tail bud areas regionally contributes to patterning was not clearly determined. We believed that if the tail bud

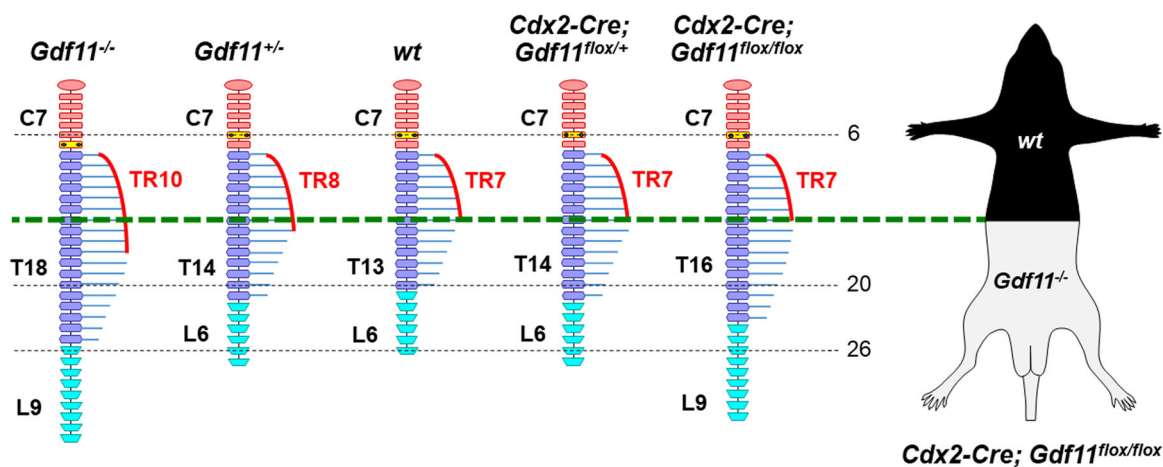


**FIGURE 4** Schematic representation of vertebral columns indicating that locally expressed GDF11, not GDF11 secreted from the tail bud, controls axial skeletal patterning. *Cdx2-Cre; Gdf11<sup>flox/flox</sup>* mice display an extended number of posterior vertebrae where GDF11 expression is removed, but normal patterning of anterior vertebrae. Cervical (orange)/thoracic (purple)/lumbar (sky blue) vertebrae, anterior tuberculi (small blue dots), sternums (red curves), and ribs (blue lines) are color-coded as indicated. Gray-dashed lines indicate normal vertebral positions: Six for the anterior tuberculum, 20 for the final thoracic vertebra, and 26 for the last lumbar vertebra. The green-dashed line represents the upper limit of *Cdx2-Cre* expression. GDF11, growth and differentiation factor 11; wt, wild-type [Color figure can be viewed at [wileyonlinelibrary.com](http://wileyonlinelibrary.com)]

truly is the major signaling center and source for GDF11, specific deletion of *Gdf11* in the tail bud would yield identical skeletal patterns to global deletion of *Gdf11*. To selectively remove *Gdf11* expression in the tail bud, we utilized a genetic approach, incorporating a *Cdx2-Cre* transgene to target recombination exclusively in the caudal region of mouse embryos harboring a floxed *Gdf11* allele. The initial screening revealed no differences in external appearance between newborn *Cdx2-Cre; Gdf11<sup>flox/flox</sup>* and *Gdf11<sup>-/-</sup>* mice, both displaying elongated trunk and shortened tail. However, closer examination uncovered disparity between their skeletal patterns; in skeletons below eighth thoracic vertebra where floxed *Gdf11* alleles are excised by *Cdx2-Cre* recombinase, *Cdx2-Cre; Gdf11<sup>flox/flox</sup>* mice exhibited anteriorly directed homeotic transformations equal to those observed in *Gdf11<sup>-/-</sup>* mice, but in skeletons above eighth thoracic vertebra where *Gdf11* is normally expressed, *Cdx2-Cre; Gdf11<sup>flox/flox</sup>* mice displayed normal skeletal patterns. In detail, characteristics of the anterior skeletons including the number of true ribs, cervical position of anterior tuberculum, and craniofacial development were all normal in *Cdx2-Cre; Gdf11<sup>flox/flox</sup>* and *Cdx2-Cre; Gdf11<sup>flox/+</sup>* mice as opposed to *Gdf11<sup>-/-</sup>* and *Gdf11<sup>+/-</sup>* mice (Figures 2, 4, and S1). Because *Cdx2-Cre; Gdf11<sup>flox/flox</sup>* mice showed skeletal defects limited to posterior regions where *Gdf11* expression is eliminated, our data suggest that GDF11, rather than globally acting as a morphogen secreted from the tail bud, locally determines the positional identity of the axial skeleton along the A–P axis.

The precise signaling mechanisms involved in local action of GDF11 during axial vertebral patterning requires further investigation. Previous studies have demonstrated that GDF11 acts upstream of *Hox* genes, regulating their expression domains, to specify regional identity of the vertebrae (Liu, 2006; McPherron et al., 1999). Indeed, expression boundaries of *Hox* genes are displaced posteriorly in mouse embryos deficient in *Gdf11* or *Pcsk5*, a gene encoding the proprotein convertase that cleaves the precursor form and activates GDF11 (Essalmani et al., 2008; McPherron et al., 1999). However, different receptors and intracellular signaling pathways utilized by GDF11 to control multiple *Hox* genes for skeletal patterning is yet to be fully elucidated. GDF11 has been shown to signal through activin type 2 receptors ACVR2A and ACVR2B, and ALK4, 5, and 7 to activate SMADs 2 and 3, which subsequently stimulate the expression of specific *Hox* genes (Andersson, Reissmann, & Ibanez, 2006; Ho, Yeo, & Whitman, 2010; Liu, 2006; Oh et al., 2002; Walker et al., 2016). GDF11 also has been reported to activate the BMP signaling pathway, phosphorylating SMADs 1, 5, and 9 (Liu, 2006; Yu et al., 2018; Zhang et al., 2016), that induces predominant expression of posterior 5' *Hox* genes (Lengerke et al., 2008; Munera et al., 2017; Seifert, Werheid, Knapp, & Tobiasch, 2015), making the *Hox* regulation by GDF11 signaling more complex. In addition, retinoic acid (RA), a morphogen, has been identified as the major initiator of anterior 3' *Hox* gene transcription as multiple anterior 3' *Hox* genes contain retinoic acid response elements (Gould, Itasaki, & Krumlauf, 1998; Packer, Crotty, Elwell, & Wolgemuth, 1998; Studer, Popperl, Marshall, Kuroiwa, & Krumlauf, 1994), and GDF11 has been shown to inactivate RA by stimulating the expression of cytochrome P450 enzyme, CYP26A1,

through ACVR2 signaling (Lee et al., 2010). Consistent with this, accumulating evidence suggests that GDF11 stimulates the expression of posterior 5' *Hox* genes, *Hox9* to *Hox13* paralogs, whereas suppressing the expression of anterior 3' *Hox* genes (Aires et al., 2016, 2019; Matsubara et al., 2017), although whether through ACVR2 signaling and inhibition of RA, or through BMP signaling is still unclear.

In the present study, we have shown that GDF11 locally regulates axial skeletal patterning rather than globally acting as a morphogen secreted from the tail bud. During embryogenesis, *Gdf11* expression level is the highest in the posterior end of the primitive streak and tail bud and gradually fades anteriorly (Figure 1a; McPherron et al., 1999; Nakashima et al., 1999). From our data, it seems likely that high expression of GDF11 in posterior ends of the embryo locally induces strong activation of posterior 5' *Hox* and inhibition of 3' *Hox* genes, coordinating the formation of posterior vertebrae, whereas mild expression of GDF11 locally regulates the positioning of relatively more anterior vertebrae through moderate activation of both posterior 5' *Hox* and anterior 3' *Hox* genes. It might be interesting to further clarify the functional relationship between local GDF11 signaling and *Hox* gene regulation during vertebral patterning in future studies.

## ACKNOWLEDGMENTS

We thank Max A. Tischfield and Jeremy Nathans for the generous gift of *Igs1<sup>CKI-mitoGFP/+</sup>* mice and Suzanne M. Sebald for assistance with shipping and handling mice. This study was supported by the Research Resettlement Fund for the new faculty of Seoul National University (to Y.-S. L.) and the National Research Foundation of Korea (Grant No. NRF-2018R1D1A1B07045334 to Y.-S. L.).

## CONFLICT OF INTERESTS

The authors declare that there are no conflict of interests.

## AUTHOR CONTRIBUTIONS

Y.-S.L. conceived and designed the study; J.S. performed most of the experiments with assistance from J.-H.E. and N.-K.K.; S.-J.L. provided most of the genetically engineered mice; J.S., K.M.W., J.-H.B., H.-M.R., and Y.-S.L. analyzed data; and J.S., S.-J.L., and Y.-S.L. wrote the paper.

## DATA AVAILABILITY STATEMENT

All data supporting the findings of this study are available within the article.

## ORCID

Joonho Suh  <http://orcid.org/0000-0003-2438-0071>

Hyun-Mo Ryoo  <http://orcid.org/0000-0001-6769-8341>

Yun-Sil Lee  <http://orcid.org/0000-0002-1228-0404>

## REFERENCES

- Agarwal, A., Wu, P. H., Hughes, E. G., Fukaya, M., Tischfield, M. A., Langseth, A. J., ... Bergles, D. E. (2017). Transient opening of the mitochondrial permeability transition pore induces microdomain calcium transients in astrocyte processes. *Neuron*, *93*(3), 587–605. <https://doi.org/10.1016/j.neuron.2016.12.034e587>
- Aires, R., Jurberg, A. D., Leal, F., Novoa, A., Cohn, M. J., & Mallo, M. (2016). Oct4 is a key regulator of vertebrate trunk length diversity. *Developmental Cell*, *38*(3), 262–274. <https://doi.org/10.1016/j.devcel.2016.06.021>
- Aires, R., deLemos, L., Novoa, A., Jurberg, A. D., Mascres, B., Duboule, D., & Mallo, M. (2019). Tail bud progenitor activity relies on a network comprising Gdf11, Lin28, and Hox13 genes. *Developmental Cell*, *48*, 383–395.e8. <https://doi.org/10.1016/j.devcel.2018.12.004>
- Andersson, O., Reissmann, E., & Ibanez, C. F. (2006). Growth differentiation factor 11 signals through the transforming growth factor-beta receptor ALK5 to regionalize the anterior-posterior axis. *EMBO Reports*, *7*(8), 831–837. <https://doi.org/10.1038/sj.embor.7400752>
- Bush, J. O., & Jiang, R. (2012). Palatogenesis: Morphogenetic and molecular mechanisms of secondary palate development. *Development*, *139*(2), 231–243. <https://doi.org/10.1242/dev.067082>
- Carapuco, M., Novoa, A., Bobola, N., & Mallo, M. (2005). Hox genes specify vertebral types in the presomitic mesoderm. *Genes and Development*, *19*(18), 2116–2121. <https://doi.org/10.1101/gad.338705>
- Essalmani, R., Zaid, A., Marcinkiewicz, J., Chamberland, A., Pasquato, A., Seidah, N. G., & Prat, A. (2008). In vivo functions of the proprotein convertase PC5/6 during mouse development: Gdf11 is a likely substrate. *Proceedings of the National Academy of Sciences of the United States of America*, *105*(15), 5750–5755. <https://doi.org/10.1073/pnas.0709428105>
- Funato, N., Nakamura, M., & Yanagisawa, H. (2015). Molecular basis of cleft palates in mice. *World Journal of Biological Chemistry*, *6*(3), 121–138. <https://doi.org/10.4331/wjbc.v6.i3.121>
- Gamer, L. W., Wolfman, N. M., Celeste, A. J., Hattersley, G., Hewick, R., & Rosen, V. (1999). A novel BMP expressed in developing mouse limb, spinal cord, and tail bud is a potent mesoderm inducer in *Xenopus* embryos. *Developmental Biology*, *208*(1), 222–232. <https://doi.org/10.1006/dbio.1998.9191>
- Gould, A., Itasaki, N., & Krumlauf, R. (1998). Initiation of rhombomeric Hoxb4 expression requires induction by somites and a retinoid pathway. *Neuron*, *21*(1), 39–51.
- Hinoi, T., Akyol, A., Theisen, B. K., Ferguson, D. O., Greenson, J. K., Williams, B. O., ... Fearon, E. R. (2007). Mouse model of colonic adenoma-carcinoma progression based on somatic Apc inactivation. *Cancer Research*, *67*(20), 9721–9730. <https://doi.org/10.1158/0008-5472.CAN-07-2735>
- Ho, D. M., Yeo, C. Y., & Whitman, M. (2010). The role and regulation of GDF11 in Smad2 activation during tailbud formation in the *Xenopus* embryo. *Mechanisms of Development*, *127*(9–12), 485–495. <https://doi.org/10.1016/j.mod.2010.08.004>
- Jurberg, A. D., Aires, R., Varela-Lasheras, I., Novoa, A., & Mallo, M. (2013). Switching axial progenitors from producing trunk to tail tissues in vertebrate embryos. *Developmental Cell*, *25*(5), 451–462. <https://doi.org/10.1016/j.devcel.2013.05.009>
- Kieny, M., Mauger, A., & Sengel, P. (1972). Early regionalization of somitic mesoderm as studied by the development of axial skeleton of the chick embryo. *Developmental Biology*, *28*(1), 142–161.
- Lee, Y. S., & Lee, S. J. (2013). Regulation of GDF-11 and myostatin activity by GASP-1 and GASP-2. *Proceedings of the National Academy of Sciences of the United States of America*, *110*(39), E3713–E3722. <https://doi.org/10.1073/pnas.1309907110>
- Lee, Y. S., & Lee, S. J. (2015). Roles of GASP-1 and GDF-11 in dental and craniofacial development. *J Oral Med Pain*, *40*(3), 110–114. <https://doi.org/10.14476/jomp.2015.40.3.110>
- Lee, Y. J., McPherron, A., Choe, S., Sakai, Y., Chandraratna, R. A., Lee, S. J., & Oh, S. P. (2010). Growth differentiation factor 11 signaling controls retinoic acid activity for axial vertebral development. *Developmental Biology*, *347*(1), 195–203. <https://doi.org/10.1016/j.ydbio.2010.08.022>
- Lengerke, C., Schmitt, S., Bowman, T. V., Jang, I. H., Maoche-Chretien, L., McKinney-Freeman, S., ... Daley, G. Q. (2008). BMP and Wnt specify hematopoietic fate by activation of the Cdx-Hox pathway. *Cell Stem Cell*, *2*(1), 72–82. <https://doi.org/10.1016/j.stem.2007.10.022>
- Liu, J. P. (2006). The function of growth/differentiation factor 11 (Gdf11) in rostrocaudal patterning of the developing spinal cord. *Development*, *133*(15), 2865–2874. <https://doi.org/10.1242/dev.02478>
- Mallo, M. (2018). Reassessing the role of Hox genes during vertebrate development and evolution. *Trends in Genetics*, *34*(3), 209–217. <https://doi.org/10.1016/j.tig.2017.11.007>
- Matsubara, Y., Hirasawa, T., Egawa, S., Hattori, A., Suganuma, T., Kohara, Y., ... Suzuki, T. (2017). Anatomical integration of the sacral-hindlimb unit coordinated by GDF11 underlies variation in hindlimb positioning in tetrapods. *Nat Ecol Evol*, *1*(9), 1392–1399. <https://doi.org/10.1038/s41559-017-0247-y>
- McPherron, A. C., Huynh, T. V., & Lee, S. J. (2009). Redundancy of myostatin and growth/differentiation factor 11 function. *BMC Developmental Biology*, *9*, 24. <https://doi.org/10.1186/1471-213X-9-24>
- McPherron, A. C., Lawler, A. M., & Lee, S. J. (1999). Regulation of anterior/posterior patterning of the axial skeleton by growth/differentiation factor 11. *Nature Genetics*, *22*(3), 260–264. <https://doi.org/10.1038/10320>
- Munera, J. O., Sundaram, N., Rankin, S. A., Hill, D., Watson, C., Mahe, M., ... Wells, J. M. (2017). Differentiation of human pluripotent stem cells into colonic organoids via transient activation of BMP signaling. *Cell Stem Cell*, *21*(1), 51–64. <https://doi.org/10.1016/j.stem.2017.05.020e56>
- Nakashima, M., Toyono, T., Akamine, A., & Joyner, A. (1999). Expression of growth/differentiation factor 11, a new member of the BMP/TGFbeta superfamily during mouse embryogenesis. *Mechanisms of Development*, *80*(2), 185–189.
- Nowicki, J. L., & Burke, A. C. (2000). Hox genes and morphological identity: Axial versus lateral patterning in the vertebrate mesoderm. *Development*, *127*(19), 4265–4275.
- Oh, S. P., Yeo, C. Y., Lee, Y., Schrewe, H., Whitman, M., & Li, E. (2002). Activin type IIA and IIB receptors mediate Gdf11 signaling in axial vertebral patterning. *Genes and Development*, *16*(21), 2749–2754. <https://doi.org/10.1101/gad.1021802>
- Packer, A. I., Crotty, D. A., Elwell, V. A., & Wolgemuth, D. J. (1998). Expression of the murine Hoxa4 gene requires both autoregulation and a conserved retinoic acid response element. *Development*, *125*(11), 1991–1998.
- Saga, Y., & Takeda, H. (2001). The making of the somite: Molecular events in vertebrate segmentation. *Nature Reviews Genetics*, *2*(11), 835–845. <https://doi.org/10.1038/35098552>
- Schilling, T. F., Nie, Q., & Lander, A. D. (2012). Dynamics and precision in retinoic acid morphogen gradients. *Current Opinion in Genetics & Development*, *22*(6), 562–569. <https://doi.org/10.1016/j.gde.2012.11.012>
- Seifert, A., Werheid, D. F., Knapp, S. M., & Tobiasch, E. (2015). Role of Hox genes in stem cell differentiation. *World Journal of Stem Cells*, *7*(3), 583–595. <https://doi.org/10.4252/wjsc.v7.i3.583>
- Silberg, D. G., Swain, G. P., Suh, E. R., & Traber, P. G. (2000). Cdx1 and cdx2 expression during intestinal development. *Gastroenterology*, *119*(4), 961–971.
- Studer, M., Popperl, H., Marshall, H., Kuroiwa, A., & Krumlauf, R. (1994). Role of a conserved retinoic acid response element in rhombomere restriction of Hoxb-1. *Science*, *265*(5179), 1728–1732.



- Tam, P. P., & Tan, S. S. (1992). The somitogenetic potential of cells in the primitive streak and the tail bud of the organogenesis-stage mouse embryo. *Development*, 115(3), 703–715.
- Tickle, C., Summerbell, D., & Wolpert, L. (1975). Positional signalling and specification of digits in chick limb morphogenesis. *Nature*, 254(5497), 199–202.
- Walker, R. G., Poggioli, T., Katsimpardi, L., Buchanan, S. M., Oh, J., Wattruss, S., ... Lee, R. T. (2016). Biochemistry and biology of GDF11 and myostatin: Similarities, differences, and questions for future investigation. *Circulation Research*, 118(7), 1125–1141. <https://doi.org/10.1161/CIRCRESAHA.116.308391discussion.1142>
- Wellik, D. M. (2007). Hox patterning of the vertebrate axial skeleton. *Developmental Dynamics*, 236(9), 2454–2463. <https://doi.org/10.1002/dvdy.21286>
- Wilson, V., Olivera-Martinez, I., & Storey, K. G. (2009). Stem cells, signals and vertebrate body axis extension. *Development*, 136(10), 1591–1604. <https://doi.org/10.1242/dev.021246>
- Wymeersch, F. J., Huang, Y., Blin, G., Cambray, N., Wilkie, R., Wong, F. C., & Wilson, V. (2016). Position-dependent plasticity of distinct progenitor types in the primitive streak. *eLife*, 5, e10042. <https://doi.org/10.7554/eLife.10042>
- Yu, X., Chen, X., Zheng, X. D., Zhang, J., Zhao, X., Liu, Y., ... Zhu, D. (2018). Growth differentiation factor 11 promotes abnormal proliferation and angiogenesis of pulmonary artery endothelial cells. *Hypertension*, 71(4), 729–741. <https://doi.org/10.1161/HYPERTENSIONAHA.117.10350>
- Zhang, Y. H., Cheng, F., Du, X. T., Gao, J. L., Xiao, X. L., Li, N., ... Dong, & de, L. (2016). GDF11/BMP11 activates both smad1/5/8 and smad2/3 signals but shows no significant effect on proliferation and migration of human umbilical vein endothelial cells. *Oncotarget*, 7(11), 12063–12074. <https://doi.org/10.18632/oncotarget.7642>

## SUPPORTING INFORMATION

Additional supporting information may be found online in the Supporting Information section.

**How to cite this article:** Suh J, Eom J-H, Kim N-K, et al. Growth differentiation factor 11 locally controls anterior–posterior patterning of the axial skeleton. *J Cell Physiol.* 2019;234:23360–23368. <https://doi.org/10.1002/jcp.28904>